Available online at www.sciencedirect.com
ScienceDirect
Catalysis Today 133–135 (2008) 600–605
CATALYSIS TODAY
www.elsevier.com/locate/cattod

Catalytic activity of an iron-pillared montmorillonitic clay mineral in heterogeneous photo-Fenton process

María A. De León [a,*], Jorge Castiglioni [a], Juan Bussi [a,b], Marta Sergio [a]

[a] *Laboratorio de Fisicoquímica de Superficies, DETEMA, Facultad de Química, Universidad de la República Oriental del Uruguay. Gral. Flores 2124, Montevideo, Uruguay*

[b] *Instituto de Ingeniería Química, Facultad de Ingeniería, Universidad de la República Oriental del Uruguay J. Herrera y Reissig 565, Montevideo, Uruguay*

Available online 13 February 2008

Abstract

Two catalysts prepared separately by iron pillaring of two different-sized particle fractions of a dried, ground and sieved clay mineral were tested for catalytic performance in photo-Fenton discoloration of methylene blue aqueous solutions.

Two different-sized particle fractions of the mineral were selected prior to pillaring, ranging below 250 μm and within the range of 250–450 μm, respectively. The resulting solids were characterized by thermogravimetric analysis, nitrogen adsorption isotherms and ultimate analysis at different preparation stages. Significant differences were found in catalyst textural parameters according to the starting mineral particle size, a higher specific surface area, and specific pore volume, was found for the catalyst obtained from the smaller-sized particle fraction of the mineral. Both catalysts showed activity in the discoloration of aqueous dye solution. Differences in catalyst performance were correlated with textural parameters. Trial tests were conducted in different experimental conditions, enabling the assessment of contributions of different catalytic mechanisms.

Keywords: Photo-Fenton; Heterogeneous catalysis; Iron-pillared clay; Methylene blue

1. Introduction

Increasing demands on environment preservation, as well as the increase in information relative to the effect of chemical products on human health, contributed to the development of cleaner technologies. These technologies aim at the replacement of contaminating processes by others that are harmless or pose no immediate threat to the environment. As the above changes in technology are taking place at a low pace, effluent treatment appears as an alternative to minimize the environmental deleterious effect of contaminating processes.

Many persistent organic chemicals in water (such as pesticides or dyes) cannot be removed by conventional biotechnological, physical or chemical processes, owing to a high operating cost and/or the production of waste water or residues that are difficult to handle [1]. As alternative methods, Advanced Oxidation Techniques (AOTs) based on the action of hydroxyl radicals ($OH^{\bullet}$) enable almost complete mineralization of organic matter using milder experimental conditions, in view of the high oxidation potential of $OH^{\bullet}$ (E^{o} = +2.8 V) [2]. One of the most important AOT processes for the generation of hydroxyl radicals is based on the combined action of Fe^{2+}/H_2O_2/UV radiation in the so called homogeneous photo-Fenton process, as Fe^{2+} ions are supplied in aqueous solution [3]. The formation of hydroxyl radicals and the regeneration of Fe^{2+} by photoreduction of Fe^{3+} may be expressed by the following equations:

$$Fe^{2+} + H_2O_2 \rightarrow Fe^{3+} + OH^{\bullet} + OH^{-} \quad (1)$$

$$H_2O_2 + h\nu \rightarrow 2OH^{\bullet} \quad (2)$$

$$Fe^{3+}(OH^{-}) + h\nu \rightarrow Fe^{2+} + OH^{\bullet} \quad (3)$$

Mazellier et al. [4] report a quantum yield of 0.07 for hydroxyl radical production by Fe^{3+} reduction at 365 nm, according to Eq. (3). In the absence of UV radiation (Fenton system),

* Corresponding author. Tel.: +598 2 9248356; fax: +598 2 9241906.
E-mail address: adeleon@fq.edu.uy (M.A. De León).

0920-5861/$ – see front matter © 2008 Elsevier B.V. All rights reserved.
doi:10.1016/j.cattod.2007.12.130

catalyst regeneration takes place through a series of reactions involving hydroperoxyl radicals ($HOO^{\bullet}$). The overall rate of regeneration and process efficiency are considerably low in these conditions.

$$Fe^{2+} + HO_2^{\bullet} \rightarrow Fe^{3+} + O_2 + H^+ \quad (4)$$

$$Fe^{3+} + H_2O_2^{\bullet} \rightarrow Fe^{2+} + HO_2^{\bullet} + H^+ \quad (5)$$

The homogeneous photo-Fenton process requires complementary steps to recover the catalyst, prevent contamination and enable catalyst re-use, such as precipitation and redissolution, the cost of the homogeneous processes thus depending largely on the supply of chemicals, power and labour requirements.

Several attempts were made to develop solid iron compounds showing catalytic activity in photo-Fenton processes [5–7]. Using simple techniques, metal oxides may be included in several widely used solids, such as smectites.

Montmorillonites constitute one of the most abundant smectitic clays in nature. They are characterized by the substitution of Al^{3+} by Mg^{2+} in the octahedral sheet, resulting in a negative layer charge that is compensated by hydrated cations adsorbed in the inter-lamellar space. These cations can be easily substituted by others present in solution. The use of bulky metallic-polioxocations was introduced by Brindley and Sempels [8] and Lahav et al. [9]. Careful calcination of the exchanged clay leads to interesting materials with permanent microporosity across a range of molecular sizes. They are reported as Pillared Inter-Layered Clays (PILCs) as the calcined oxocations act as pillars that prop up clay layers. Different oxocations containing Al, Zr, Ti, La, Ga, Fe or Cr have since then been used. Several reviews have reported on the subject [10–13]. PILCs are attractive as adsorbents, catalysts or catalyst support due to their high specific surface area [14,15]. PILCs prepared with iron oxocations (Fe-PILC) have recently been used in dye mineralization [16–18] using photo-Fenton techniques.Conventional methods use a mineral's clay fraction (<2 μm) for the preparation of PILCs. The separation of the clay fraction from the starting raw mineral being an expensive and time-consuming process, a new strategy was developed in this study for Fe-PILC preparation. A montmorillonitic clay mineral abundant in Uruguay was pillared without any further pre-treatment than drying, grinding and sieving. Two different particle-sized fractions were exchanged with iron oxocations and calcined to yield Fe-PILC. The catalytic activity of the resulting solids was tested in discoloration of methylene blue (Mb) aqueous solution under experimental condition similar to those of the photo-Fenton system.

2. Experimental

2.1. Catalyst preparation

A clay mineral collected from Bañado de Medina, Uruguay, was used as starting raw material. The mineral contains more than 80% of a calcium-rich montmorillonite with low Na^+ and K^+ content [19]. Cation-exchange capacity (CEC) of the mineral determined by the ammonium acetate method (1 M, pH 7) was 107 meq/100 g of dry mineral. The raw material was dried, ground in a Ketshmühle (WRb 90 lb/4p) mill and sieved. The particle size fraction ranging less than 250 μm ($M_{<250}$) and the fraction in the range of 250–450 μm ($M_{250–450}$) were used for Fe-PILC preparation.

Tri-nuclear ferric acetate complex ion – $[Fe_3(OCO\text{-}CH_3)_7OH{\cdot}2H_2O]NO_3$ – was prepared according to the method described by Yamanaka et al. [20]: 40.4 g of $Fe(NO_3)_3$ were dissolved in 25 mL of ethyl alcohol, followed by the addition of 70 mL of acetic anhydride in small portions. The reacting system was kept in ice bath and the precipitate was separated by filtration. Without further treatment, the solid was used to prepare a 0.05 M aqueous solution of Fe(III) complex-ion.

Suspensions (10% by weight) of both mineral particle size fractions were prepared using distilled water and a volume of the Fe(III) complex ion solution was added to obtain 3.5 mol of the ferric ion per gram of mineral; the resulting suspensions were aged under stirring for 3 h at 40 °C and for 18 h at room temperature. The exchanged minerals (EMs) were recovered by filtration, washed with deionized water until constant conductivity of residual wash-water. The solids were oven-dried at 50 °C and labeled according to the starting mineral particle fraction as $EM_{<250}$ or $EM_{250–450}$.

The EM samples were calcined in a tubular furnace Carbolite CTF-12/65/550 at a heating rate of 1 °C/min up to 400 °C, which was kept constant for 2 h. The catalysts thus obtained were identified as Fe-$PILC_{<250}$ and Fe-$PILC_{250–450}$.

2.2. Catalyst characterization

Ultimate analysis of the starting mineral (EMs) was performed using Carlo Erba EA1108 CHNS-0 equipment.

Thermogravimetric analysis (TGA) of EM samples was performed in Shimadzu TGA-50 equipment. Samples were heated up to 500 °C at a heating rate of 10 °C/min in a platinum capsule, at an airflow rate of 50 mL/min.

Nitrogen adsorption–desorption isotherms were determined at −196 °C in Autosorb-1 (Quantachrome) equipment. Fe-PILCs were outgassed under vacuum at 250 °C for 4 h (final pressure was below 10^{-4} mbar). Textural parameters were derived from the adsorption data. The specific surface area was determined from the isotherms using the BET model (S_{BET}), obtaining a good fit in the range of relative pressures of 0.07–0.1. Specific total pore volume (V_T) was determined from the adsorbed volume at a relative pressure of 0.95 assuming a density of 0.808 g/mL for the adsorbed nitrogen. Specific micropore volume ($V_{\mu p}$) was determined using the Dubinin–Radushkevich model and the external specific surface area by application of *t*-plot diagrams to data through the 0.85–0.95 range of relative pressures [21].

2.3. Photo-catalytic reactor

A batch photo-reactor (Fig. 1) consisting of a borosilicate glass tube having a sintered glass piece placed at the bottom was used. Four UV lamps, Phillips TLD 18 W (maximum of the

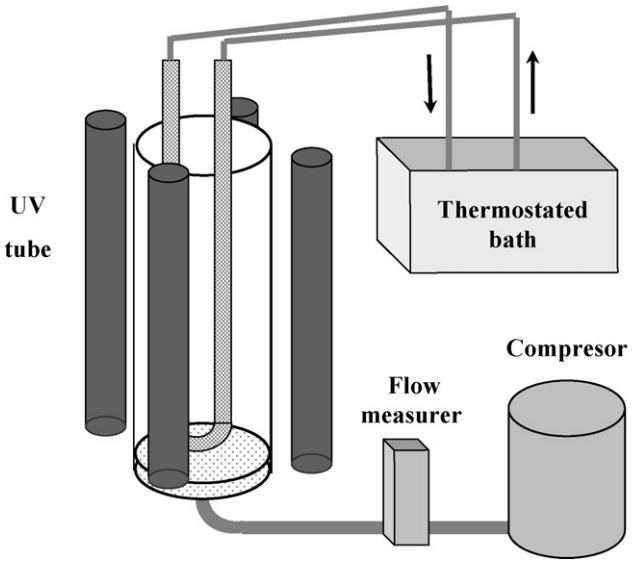

Fig. 1. Schematic diagram of the photo-catalytic reactor used in this study.

spectrum at 360 nm) were placed around the reactor and an external aluminum foil (not shown in the figure) was used to prevent scattered radiation. An U-shaped tube was placed in the center of the reactor for temperature control. A circulation pump and a thermostated water bath (27 ± 0.5 °C) were used for this purpose. To ensure adequate suspension of the catalyst, air bubbling was used by injection of compressed air through the sintered glass in the bottom of the reactor, adjusting the air flow rate to 1.5 L/min using a mass flow controller Omega FMA 1412.

2.4. Photo-catalytic experiments

The photo-catalytic activity of Fe-PILCs was evaluated in discoloration of Mb aqueous solutions in the presence of H_2O_2 and UV radiation. Remnant Mb in solution was determined using a SHIMADZU spectrophotometer UV-1201V. Absorbance measurements were recorded at 665 nm, corresponding to the maximum in the Mb absorption spectrum.

In the basic photo-Fenton experiment, 0.5 L of the reactant solution (0.2 mM in Mb and 10 mM in H_2O_2) were poured into the reactor, and once the air flow was started, 0.5 g of the catalyst were added and pH was adjusted to 3.0 with dilute HCl solution. The importance of different factors involved in the process (catalyst, H_2O_2, pH adjustment and UV radiation) was studied by assaying individual parameters.

A blank experiment to characterize dye adsorption on the catalyst was performed in the reactor using exclusively the catalyst and the Mb solution.

3. Results and discussion

3.1. Catalyst characterization

Ultimate analysis of dried clay mineral samples ($M_{<250}$ and $M_{250–450}$) indicated the absence of significant amounts of carbon. The carbon content of the dried exchanged

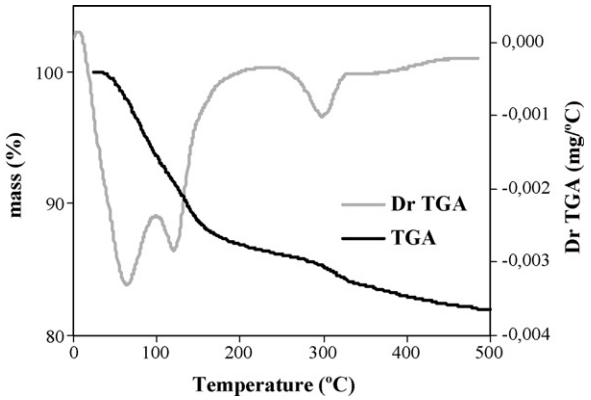

Fig. 2. Thermogravimetric analysis of $EM_{<250}$.

iron-complex samples, $EM_{<250}$ and $EM_{250–450}$, was 1.3% and 1.1%, respectively, confirming the inclusion of the tri-nuclear ferric acetate complex. Further, as the molecular formula of the iron complex, $[Fe_3(OCOCH_3)_7OH{\cdot}2H_2O]NO_3$, defines a stoichiometric Fe/C mass ratio of 0.997, it is possible to calculate the mass of incorporated iron in the mineral sample, the included iron content being 18% higher for $EM_{<250}$ (1.3% and 1.1% for $EM_{<250}$ and $EM_{250–450}$, respectively).

Thermogravimetric analysis results for the exchanged mineral samples, $EM_{<250}$ and $EM_{250–450}$, are shown in Figs. 2 and 3, respectively. Both diagrams show an important weight loss in the range of 40–170 °C, consistently with a variation in the derivative thermal analysis (DrTGA). A second weight loss and a peak in the DrTGA were found at higher temperatures, in the range of 260–350 °C. Sample mass remained practically constant in the range of 350–500 °C. The first weight loss, amounting to 19.6% for $EM_{<250}$ and 12.1% for $EM_{250–450}$, was attributed to desorption of physisorbed water from the sample surface and to the release of water from the inter-layer space [20,22]. The second weight loss was attributed to the decomposition and oxidation of acetyl groups, resulting in the formation of Fe_2O_3 pillars in the inter-lamellar space, the loss for $EM_{<250}$ and $EM_{250–450}$, respectively amounting to 3.6% and 2.9% of the sample mass at 400 °C (calcination temperature). Thus, the mass lost due

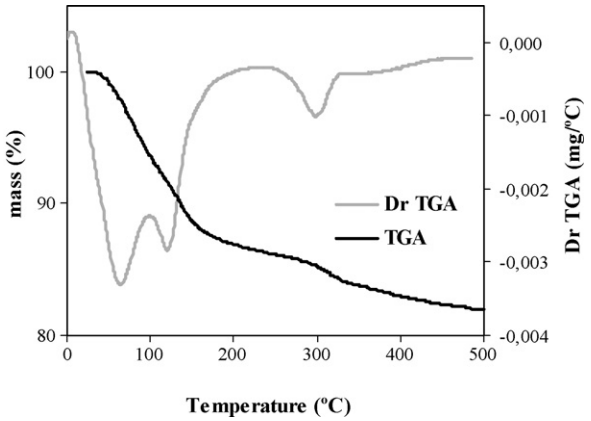

Fig. 3. Thermogravimetric analysis of $EM_{250–450}$.

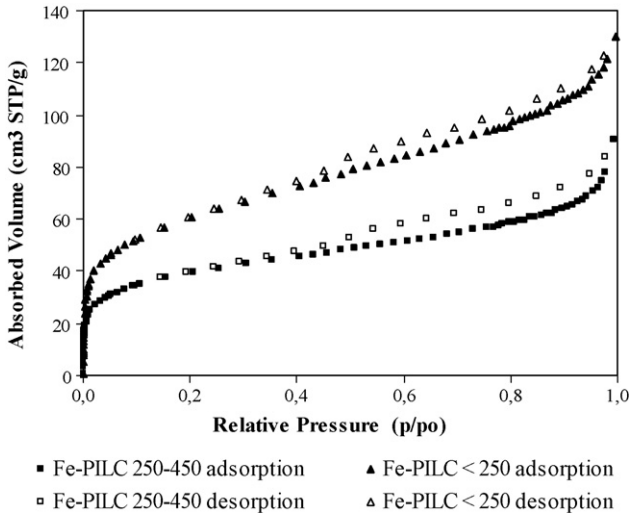

Fig. 4. Nitrogen adsorption-desorption isotherms for Fe-PILC catalysts.

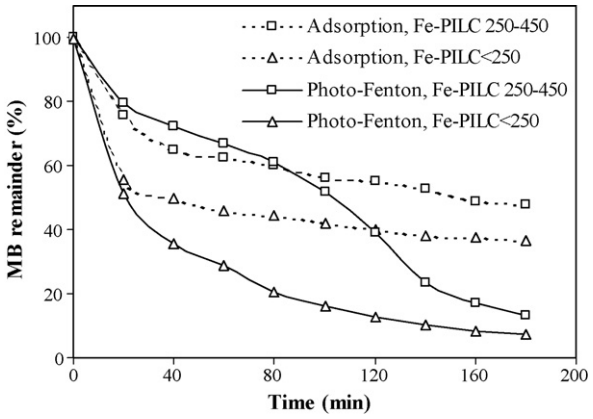

Fig. 5. Mb adsorption and Mb removal by photo-Fenton process for Fe-PILC$_{<250}$ and Fe-PILC$_{250–450}$ catalysts.

to decomposition of acetyl groups was 20% higher for the exchanged mineral of smaller particle size, a similar result to that obtained by ultimate analysis.

Fe-PILC$_{<250}$ and Fe-PILC$_{250–450}$ nitrogen adsorption–desorption isotherms are shown in Fig. 4. Both catalysts showed significant adsorption at very low relative pressures, characteristic of microporous solids. In addition, they exhibited a small H-type hysteresis cycle [21] characteristic of solids with flat particles, like the materials here studied. The pillared mineral Fe-PILC$_{<250}$, prepared with the smaller-sized mineral fraction showed higher adsorption at low relative pressures, indicating a greater specific micropore volume. Isotherms are not parallel in the higher relative pressure region. The slightly larger slope for the Fe-PILC$_{<250}$ isotherm is consistent with a larger specific external area determined from the *t*-plot diagram (Table 1). These observations are also in agreement with the different specific total pore volume and specific mesopore volume of both samples. This suggests that the inter-particle space is responsible for mesopore adsorption, which is also consistent with a similar correspondence reported by Sergio et al. [23] between textural properties of Al-PILCs and the mineral particle size of the starting material.

Textural parameters of catalysts determined from nitrogen adsorption data are summarized in Table 1. Fe-PILC obtained using the smaller-sized fraction showed a higher value of specific surface area and specific total and micropore volumes than the analogous Fe-PILC$_{250–450}$ values by a ratio in no case smaller than 50%. The specific external surface area was also higher for Fe-PILC$_{<250}$.

Table 1
Textural parameters for Fe-PILCs catalysts

	S_{BET} (m^2/g)	$V_{\mu p}$ (cm^3/g)	V_T (cm^3/g)	S_{ext} (m^2/g)
Fe-PILC$_{<250}$	212	0.09	0.18	34
Fe-PILC$_{250–450}$	140	0.06	0.11	26

3.2. Photo-catalytic experiments

In the absence of catalyst (H_2O_2, UV radiation, pH 3.0) no significant discoloration of the Mb solution was observed. While other authors reported the photochemical formation of hydroxyl radicals at 254 nm UV radiation and in the absence of iron species, a larger wavelength used in this study may be responsible for discrepancies.

Results of catalytic activity tests for Fe-PILC$_{<250}$ and Fe-PILC$_{250–450}$ in Mb discoloration are shown in Fig. 5. Adsorption tests (in the presence of catalyst and in the absence of light and H_2O_2) showed a rapid initial reduction of Mb concentration in solution, for both catalysts. The adsorption rate decreases significantly towards the end of the test as the system approaches an adsorption equilibrium. Methylene blue removal due to adsorption was as high as 52% of the dye amount for Fe-PILC$_{250–450}$ and 63% for Fe-PILC$_{<250}$. The higher adsorption found for Fe-PILC$_{<250}$ may be correlated to a higher specific surface area for this sample.

Results of the photo-Fenton experiment (Fig. 5) for Fe-PILCs clearly evidence the combined effect of catalyst, UV radiation, H_2O_2 and pH on solution discoloration. Mb removal in the assayed conditions was as high as 93% for Fe-PILC$_{<250}$ and 87% for Fe-PILC$_{250–450}$, i.e. higher than those obtained in adsorption assays. The evolution of Mb concentration was found to differ considerably for both catalysts. A coincidence between adsorption and photo-Fenton curves during the first 20 min of the assay suggests no contribution of the phenomenon promoted by light and H_2O_2 over this period. The contribution of the photo-catalytic process for the Fe-PILC$_{<250}$ catalyst becomes noticeable after 20 min of reaction, as it is evidenced by the higher curve slope (removal rate) compared to those of the adsorption experiment. In the range 20–80 min, the photo-Fenton curve for Fe-PILC$_{250–450}$ runs slightly above that of the adsorption assay. This situation is reverted after 80 min, and practically total dye removal is attained in 180 min. An inflexion point in the curve of the catalyst with lower iron content may be attributable to the competition of reactants for the active sites. Consistently with this hypothesis, the above-described pattern was not found for Fe-PILC$_{<250}$, having a higher iron content.

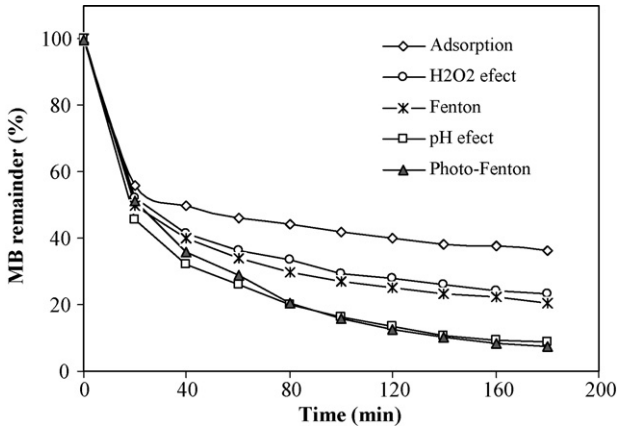

Fig. 6. UV, H_2O_2 and pH effect in photo-Fenton process for Fe-PILC$_{<250}$ catalyst. Adsorption: Mb, pH = 3. H_2O_2 effect: Mb, pH = 3, UV. Fenton: Mb, pH = 3, H_2O_2. pH effect: Mb, pH = 5.6, H_2O_2, UV. Photo-Fenton: Mb, pH = 3, H_2O_2, UV.

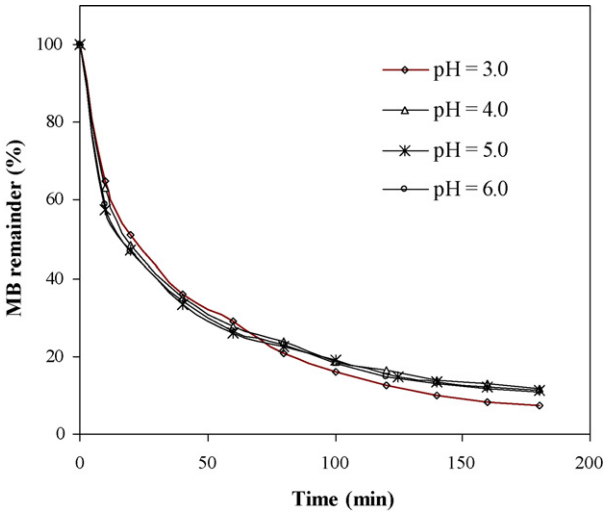

Fig. 7. pH effect on photo-Fenton experiment using Fe-PILC$_{<250}$ catalyst.

In order to study the individual contribution of UV radiation, H_2O_2 concentration and pH, complementary assays were performed. Fe-PILC$_{<250}$ was used in these assays in view of its higher catalytic activity. Results are shown in Fig. 6. Adsorption and photo-Fenton curves are also included for comparison purposes. In the Fenton assay (catalyst, H_2O_2 and pH 3.0) Mb removal was higher than in the adsorption assay, but significantly lower than for the photo-Fenton assay, using UV radiation. These results suggest that both Fenton and photo-Fenton processes contribute to hydroxyl radicals formation.

In the absence of UV radiation (Fenton system) the catalytic decomposition of hydrogen peroxide over solid iron oxide catalysts was proposed by Lin et al. [24] to take place through the formation of peroxide complex species on the Fe(III) active sites. A series of reactions involving electron transfer generate active Fe(II) species and hydroperoxyl radicals. Reduced iron sites may react with either hydrogen peroxide or oxygen, thus reoxidizing iron. The additional presence of UV radiation (photo-Fenton system) accelerates hydroxyl radical formation possibly by photoreduction of Fe(III) active sites, in a similar manner as proposed for the homogeneous process. Further reaction of Mb adsorbed on the surface of Fe-PILC with hydroxyl radicals may lead to the formation of reaction intermediates and eventually to CO_2 and H_2O as final products. Strong adsorption of the organic reactant seems to be a necessary condition for reaction to take place. Indeed, unpublished results obtained in our laboratory indicate that degradation is extremely poor for organic compounds exhibiting no significant chemisorption on the Fe-PILCs, even in the presence of UV radiation (photo-Fenton system).

Results of tests on the effect of H_2O_2 (catalyst, UV radiation and pH 3.0) showed that Mb discoloration took place even in the absence of H_2O_2; catalytic activity was found to be of the same order as for the Fenton assay. In these conditions, the formation of $OH^{\bullet}$ could take place directly from photoactive Fe(III) hydroxycomplexes on the surface of Fe-PILC, as described in Eq. (3) for the homogeneous system. Reoxidation of Fe(II) by oxygen has been suggested to take place according to the following equations [24]:

$$\mathrm{Fe(II)} + \mathrm{O_2} + \mathrm{H_2O} \rightarrow \mathrm{Fe(III)(OH)^{2+}} + \mathrm{HO_2^{\bullet}} \quad (6)$$

$$2\mathrm{HO_2^{\bullet}} \rightarrow \mathrm{H_2O_2} + \mathrm{O_2} \quad (7)$$

In the presence of semiconductor metal oxides such as TiO_2, ZnO and Fe_2O_3 [25], $OH^{\bullet}$ are known to generated by photoactivation mechanisms involving the formation of e^-–h^+ pairs. The presence of Fe_2O_3 with a tetragonal structure in iron-pillared laponite prepared by similar procedures as used in this study is reported in the literature [26].

In order to evaluate the effect of pH in the photo-Fenton process, the system was assayed without the addition of HCl. pH was therefore 5.6. Results were similar to those of the photo-Fenton assay performed at pH 3.0, suggesting a wide pH range of effectiveness for the heterogeneous process. Further experiments with pH ranging from 3.0 to 6.0 (Fig. 7) are consistent with this assumption. Therefore, even though efficient photolysis of $Fe(OH)^{2+}$ species is favored at pH 3 in the homogeneous photo-Fenton process [27], the influence of pH may be attenuated in the heterogeneous system since immobilized Fe(III) species could not be transformed into less photoactive materials: $Fe^{3+}(H_2O)_6$ at lower pH and $Fe(OH)_3$ at higher pH, as in the homogeneous system. Further, the stabilization of iron oxide pillars may also be attributable to interactions with the clay sheet.

4. Conclusions

Both catalysts prepared by iron pillaring of different-sized particle fractions of a Uruguayan clay mineral proved to be microporous solids with a high specific surface area and considerable photo-Fenton catalytic activity. An improvement of catalyst textural parameters and an increase in catalytic activity in methylene blue discoloration by photo-Fenton processes was found for the smaller-sized particle fraction of the starting mineral. Under reaction conditions used in this study, the formation of hydroxyl radicals is promoted through

different mechanisms involving red–ox interactions between H_2O_2 and iron (Fenton type reactions) as well as UV radiation (photo-Fenton) or between different adsorbed species and e^-–h^+ photo-generated pairs. As in homogenous Fenton reactions, the presence of light increases the rate of formation of species leading to the generation of radicals.

Further research should enable the assessment of feasibility for the application of the Fe-PILC catalyst to the depletion of different residual water polluting agents.

Acknowledgements

''Comisión Sectorial de Investigación Científica'' (CSIC) of the University of Uruguay, and ''Programa de Desarrollo de las Ciencias Básicas (PEDECIBA)'' for financial support. Dra. Lucía Otero for the conduction of ultimate analysis. Chem. Eng. Eduardo Speranza for edition of the English manuscript.

References

[1] P.K. Malik, S.K. Saha, Sep. Purif. Technol. 31 (2003) 241.
[2] O. Legrine, E. Oliveros, A.M. Braun, Chem. Rev. 93 (1993) 671.
[3] J.J. Pignatello, D. Liu, P. Huston, Environ. Sci. Technol. 33 (1999) 1832.
[4] P. Mazellier, G. Mailhot, M. Bolte, New J. Chem. 21 (1997) 389.
[5] J. Feng, X. Hu, P.L. Yue, H.Y. Zhu, G.Q. Lu, Ind. Eng. Chem. Res. 42 (2003) 2066.
[6] F. Martínez, G. Calleja, J.A. Melero, R. Molina, Appl. Catal. B: Environ. 60 (2005) 181.
[7] M. Noorjahan, V. Durga Kumari, M. Subrahmanyam, L. Panda, Appl. Catal. B: Environ. 57 (2005) 291.
[8] G.M. Brindley, R.E. Sempels, Clay Miner. 12 (1977) 229.
[9] N. Lahav, V. Shani, J. Shabtai, Clays Clay Miner. 26 (1978) 107.
[10] R. Burch (Ed.), Pillared Clays. Special Issue. Catalysis Today, vol. 2, Elsevier Science Pub. B.V, Amsterdam, 1988, pp. 185–368.
[11] F. Figueras, Catal. Rev. Sci. Eng. 30 (1988) 457.
[12] J.T. Kloprogge, J. Porous Mater. 5 (1998) 5.
[13] A. Gil, L. Gandía, M. Vicente, Catal. Rev-Sci. Eng. 42 (1&2) (2000) 145.
[14] T.J. Pinnavaia, Science 220 (1983) 365.
[15] R.M. Barrer, J. Inclusion Phenom. 4 (1977) 109.
[16] J. Feng, X. Hu, P.L. Yue, Environ. Sci. Technol. 38 (2004) 269.
[17] J. Feng, X. Hu, P.L. Yue, Water Res. 40 (2006) 641.
[18] Y. Li, Y. Lu, X. Zhu, J. Hazard. Mater. 132 (2006) 196.
[19] I. Ford, M. Sergio, Boletín de Informaciones, Fac. de Agronomía, UDELAR, 23 (1989).
[20] S. Yamanaka, T. Doi, S. Sako, M. Hattori, Mater. Res. Bull. 19 (1984) 161.
[21] S.J. Gregg, K.S.W. Sing, Adsorption Surface Area and Porosity, Academic Press, London, U.K., 1982.
[22] T. Mishra, K.M. Parida, S.B. Rao, J. Colloid Interface Sci. 183 (1996) 176.
[23] M. Sergio, M. Musso, J. Medina, W. Diano, Adv. Tech. Mater. Mater. Proc. J. 8 (2006) 5.
[24] S.S. Lin, M.D. Gurol, Environ. Sci. Technol. 32 (1998) 1417.
[25] J. Bandara, J.A. Mielczarski, A. López, J. Appl. Catal. B: Environ. 34 (2001) 321.
[26] J. Feng, X. Hu, P.L. Yue, H.Y. Zhu, G.Q. Lu, Water Res. 37 (2003) 3776.
[27] J.J. Pignatello, Environ. Sci. Technol. 26 (1992) 944.